cut into an absorbing material and placed one at the beginning and one at the end of a collimating distance L. The maximum beam divergence that is transmitted with this configuration is

$$\alpha_{\max} = (a_1 + a_2)/L, \qquad (4.4.2.1)$$

where a_1 and a_2 are the widths of the slits or pinholes.

Such a device is normally used for small-angle scattering and reflectometry. In order to avoid parasitic scattering by reflection from slit edges, very thin sheets of a highly absorbing material, *e.g.* gadolinium foils, are used as the slit material. Sometimes wedge-formed cadmium plates are sufficient. In cases where a very precise edge is required, cleaved single-crystalline absorbers such as gallium gadolinium garnet (GGG) can be employed.

To avoid high intensity losses when the distances are large, sections of neutron guide can be introduced between the collimators, as in, for example, small-angle scattering instruments with variable collimation. In this case, for maximum intensity at a given resolution (divergence), the collimator length should be equal to the camera length, *i.e.* the sample–detector distance (Schmatz, Springer, Schelten & Ibel, 1974).

As can be seen from (4.4.2.1), the beam divergence from a simple slit or pinhole collimator depends on the aperture size. In order to collimate (in one dimension) a beam of large cross section within a reasonable distance L, Soller collimators, composed of a number of equidistant neutron absorbing blades, are used. To avoid losses, the blades must be as thin and as flat as possible. If their surfaces do not reflect neutrons, which can be achieved by using blades with rough surfaces or materials with a negative scattering length, such as foils of hydrogen-containing polymers (Mylar is commonly used) or paper coated with neutron-absorbing paint containing boron or gadolinium (Meister & Weckerman, 1973; Carlile, Hey & Mack, 1977), the angular dependence of the transmission function is close to the ideal triangular form, and transmissions of 96% of the theoretical value can be obtained with 10′ collimation. If the blades of the Soller collimator are coated with a material whose critical angle of reflection is equal to $\alpha_{\max}/2$ (for one particular wavelength), then a square angular transmission function is obtained instead of the normal triangular function, thus doubling the theoretical transmission (Meardon & Wroe, 1977).

Soller collimators are often used in combination with single-crystal monochromators to define the wavelength resolution of an instrument but the Soller geometry is only useful for one-dimensional collimation. For small-angle scattering applications, where two-dimensional collimation is required, a converging 'pepper pot' collimator can be used (Nunes, 1974; Glinka, Rowe & LaRock, 1986).

Cylindrical collimators with radial blades are sometimes used to reduce background scattering from the sample environment. This type of collimator is particularly useful with position-sensitive detectors and may be oscillated about the cylinder axis to reduce the shadowing effect of the blades (Wright, Berneron & Heathman, 1981).

4.4.2.3. *Crystal monochromators*

Bragg reflection from crystals is the most widely used method for selecting a well defined wavelength band from a white neutron beam. In order to obtain reasonable reflected intensities and to match the typical neutron beam divergences, crystals that reflect over an angular range of 0.2 to 0.5° are typically employed. Traditionally, mosaic crystals have been used in preference to perfect crystals, although reflection from a mosaic crystal gives rise to an increase in beam divergence with a concomitant broadening of the selected wavelength band. Thus, collimators are often used together with mosaic monochromators to define the initial and final divergences and therefore the wavelength spread.

Because of the beam broadening produced by mosaic crystals, it was soon recognised that elastically deformed perfect crystals and crystals with gradients in lattice spacings would be more suitable candidates for focusing applications since the deformation can be modified to optimize focusing for different experimental conditions (Maier-Leibnitz, 1969).

Perfect crystals are used commonly in high-energy-resolution backscattering instruments, interferometry and Bonse–Hart cameras for ultra-small-angle scattering (Bonse & Hart, 1965).

An ideal mosaic crystal is assumed to comprise an agglomerate of independently scattering domains or mosaic blocks that are more or less perfect, but small enough that primary extinction does not come into play, and the intensity reflected by each block may be calculated using the kinematic theory (Zachariasen, 1945; Sears, 1997). The orientation of the mosaic blocks is distributed inside a finite angle, called the mosaic spread, following a distribution that is normally assumed to be Gaussian. The ideal neutron mosaic monochromator is not an ideal mosaic crystal but rather a mosaic crystal that is sufficiently thick to obtain a high reflectivity. As the crystal thickness increases, however, secondary extinction becomes important and must be accounted for in the calculation of the reflectivity. The model normally used is that developed by Bacon & Lowde (1948), which takes into account strong secondary extinction and a correction factor for primary extinction (Freund, 1985). In this case, the mosaic spread (usually defined by neutron scatterers as the full width at half maximum of the reflectivity curve) is not an intrinsic crystal property, but increases with wavelength and crystal thickness and can become quite appreciable at longer wavelengths.

Ideal monochromator materials should have a large scattering-length density, low absorption, incoherent and inelastic cross sections, and should be available as large single crystals with a suitable defect concentration. Relevant parameters for some typical neutron monochromator crystals are given in Table 4.4.2.1.

In principle, higher reflectivities can be obtained in neutron monochromators that are designed to operate in reflection geometry, but, because reflection crystals must be very large when takeoff angles are small, transmission geometry may be used. In that case, the optimization of crystal thickness can only be achieved for a small wavelength range.

Nickel has the highest scattering-length density, but, since natural nickel comprises several isotopes, the incoherent cross section is quite high. Thus, isotopic ^{58}Ni crystals have been grown as neutron monochromators despite their expense. Beryllium, owing to its large scattering-length density and low incoherent and absorption cross sections, is also an excellent candidate for neutron monochromators, but the mosaic structure of beryllium is difficult to modify, and the availability of good-quality single crystals is limited (Mücklich & Petzow, 1993). These limitations may be overcome in the near future, however, by building composite monochromators from thin beryllium blades that have been plastically deformed (May, Klimanek & Magerl, 1995).

Pyrolytic graphite is a highly efficient neutron monochromator if only a medium resolution is required (the minimum mosaic spread is of the order of 0.4°), owing to high reflectivities, which may exceed 90% (Shapiro & Chesser, 1972), but its use is limited to wavelengths above 1.5Å, owing to the rather large d spacing of the 002 reflection. Whenever better resolution at

Table 4.4.2.1. *Some important properties of materials used for neutron monochromator crystals (in order of increasing unit-cell volume)*

Material	Structure	Lattice constant(s) at 300 K a, c (Å)	Unit-cell volume $V_0(10^{-24}$ cm$^3)$	Coherent scattering length b (10^{-12} cm)	Square of scattering-length density 10^{-21} cm^{-4}	Ratio of incoherent to total scattering cross section $\sigma_{\rm inc}/\sigma_s$	Absorption cross section $\sigma_{\rm abs}$ (barns)* (at $\lambda = 1.8$ Å)	Atomic mass A	Debye temperature θ_D (K)	$A\theta_D^2$ (10^6 K^2)
Beryllium	h.c.p	a : 2.2856 c : 3.5832	16.2	0.779 (1)	9.25	6.5×10^{-4}	0.0076 (8)	9.013	1188	12.7
Iron	b.c.c.	a : 2.8664	23.5	0.954 (6)	6.59	0.033	2.56 (3)	55.85	411	9.4
Zinc	h.c.p.	a : 2.6649 c : 4.9468	30.4	0.5680 (5)	1.50	0.019	1.11 (2)	65.38	253	4.2
Pyrolytic graphite	layer hexag.	a : 2.461 c : 6.708	35.2	0.66484 (13)	5.71	$< 2 \times 10^{-4}$	0.00350 (7)	12.01	800	7.7
Niobum	b.c.c.	3.3006	35.9	0.7054 (3)	1.54	4×10^{-4}	1.15 (5)	92.91	284	7.5
Nickel (^{58}Ni)	f.c.c.	3.5241	43.8	1.44 (1)	17.3	0	4.6 (3)	58.71	417	9.9
Copper	f.c.c.	3.6147	47.2	0.7718 (4)	4.28	0.065	3.78 (2)	63.54	307	6.0
Aluminium	f.c.c.	4.0495	66.4	0.3449 (5)	0.43	5.6×10^{-3}	0.231 (3)	26.98	402	4.4
Lead	f.c.c.	4.9502	121	0.94003 (14)	0.97	2.7×10^{-4}	0.171 (2)	207.21	87	1.6
Silicon	diamond	5.4309	160	0.41491 (10)	0.43	6.9×10^{-3}	0.171 (3)	28.09	543	8.3
Germanium	diamond	5.6575	181	0.81929 (7)	1.31	0.020	2.3 (2)	72.60	290	6.1

* 1 barn= 10^{-28} m^2.

shorter wavelengths is required, copper (220 and 200) or germanium (311 and 511) monochromators are frequently used. The advantage of copper is that the mosaic structure can be easily modified by plastic deformation at high temperature. As with most face-centred cubic crystals, it is the (111) slip planes that are functional in generating the dislocation density needed for the desired mosaic spread, and, depending on the required orientation, either isotropic or anisotropic mosaics can be produced (Freund, 1976). The latter is interesting for vertical focusing applications, where a narrow vertical mosaic is required regardless of the resolution conditions.

Although both germanium and silicon are attractive as monochromators, owing to the absence of second-order neutrons for odd-index reflections, it is difficult to produce a controlled uniform mosaic spread in bulk samples by plastic deformation at high temperature because of the difficulty in introducing a spatially homogenous microstructure in large single crystals (Freund, 1975). Recently this difficulty has been overcome by building up composite monochromators from a stack of thin wafers, as originally proposed by Maier-Leibnitz (1967; Frey, 1974).

In practice, an artificial mosaic monochromator can be built up in two ways. In the first approach, illustrated in Fig. 4.4.2.1(*a*), the monochromator comprises a stack of crystalline wafers, each of which has a mosaic spread close to the global value required for the entire stack. Each wafer in the stack must be plastically deformed (usually by alternated bending) to produce the correct mosaic spread. For certain crystal orientations, the plastic deformation may result in an anisotropic mosaic spread. This method has been developed in several laboratories to construct germanium monochromators (Vogt, Passell, Cheung & Axe, 1994; Schefer *et al.*, 1996).

In the second approach, shown in Fig. 4.4.2.1(*b*), the global reflectivity distribution is obtained from the contributions of several stacked thin crystalline wafers, each with a rather narrow mosaic spread compared with the composite value but slightly misoriented with respect to the other wafers in the stack. If the misorientation of each wafer can be correctly controlled, this technique has the major advantage of producing monochromators with a highly anisotropic mosaic structure. The shape of the reflectivity curve can be chosen at will (Gaussian, Lorentzian, rectangular), if required. Moreover, because the initial mosaicity required is small, it is not necessary to use mosaic wafers and therefore for each wafer to undergo a long and tedious plastic deformation process. Recently, this method has been applied successfully to construct copper monochromators (Hamelin, Anderson, Berneron, Escoffier, Foltyn & Hehn, 1997), in which individual copper wafers were cut in a cylindrical form and then slid across one another to produce the required mosaic spread in the scattering plane. This technique looks very promising for the production of anisotropic mosaic monochromators.

The reflection from a mosaic crystal is visualized in Fig. 4.4.2.2(*b*). An incident beam with small divergence is transformed into a broad exit beam. The range of **k** vectors, Δk, selected in this process depends on the mosaic spread, η, and the incoming and outgoing beam divergences, α_1 and α_2.

$$\Delta k/k = \Delta\tau/\tau + \alpha \cot\theta, \tag{4.4.2.2}$$

where τ is the magnitude of the crystal reciprocal-lattice vector ($\tau = 2\pi/d$) and α is given by

$$\alpha = \sqrt{\frac{\alpha_1^2\alpha_2^2 + \alpha_1^2\eta^2 + \alpha_2^2\eta^2}{\alpha_1^2 + \alpha_2^2 + 4\eta^2.}} \tag{4.4.2.3}$$

The resolution can therefore be defined by collimators, and the highest resolution is obtained in backscattering, where the wavevector spread depends only on the intrinsic $\Delta d/d$ of the crystal.

In some applications, the beam broadening produced by mosaic crystals can be detrimental to the instrument performance. An interesting alternative is a gradient crystal, *i.e.* a single crystal with a smooth variation of the interplanar lattice spacing along a defined crystallographic direction. As shown in Fig. 4.4.2.2(*c*), the diffracted phase-space element has a different shape from that obtained from a mosaic crystal. Gradients in d spacing can be produced in various ways,

including thermal gradients (Alefeld, 1972), vibrating crystals by piezoelectric excitation (Hock, Vogt, Kulda, Mursic, Fuess & Magerl, 1993), and mixed crystals with concentration gradients, *e.g.* Cu–Ge (Freund, Guinet, Maréschal, Rustichelli & Vanoni, 1972) and Si–Ge (Maier-Leibnitz & Rustichelli, 1968; Magerl, Liss, Doll, Madar & Steichele, 1994).

Both vertically and horizontally focusing assemblies of mosaic crystals are employed to make better use of the neutron flux when making measurements on small samples. Vertical focusing can lead to intensity gain factors of between two and five without affecting resolution (real-space focusing) (Riste, 1970; Currat, 1973). Horizontal focusing changes the k-space volume that is selected by the monochromator through the variation in Bragg angle across the monochromator surface (k-space focusing) (Scherm, Dolling, Ritter, Schedler, Teuchert & Wagner, 1977). The orientation of the diffracted k-space volume can be modified by variation of the horizontal curvature, so that the resolution of the monochromator may be optimized with respect to a particular sample or experiment without loss of illumination. Monochromatic focusing can be achieved. Furthermore, asymmetrically cut crystals may be used, allowing focusing effects in real space and k space to be decoupled (Scherm & Kruger, 1994).

Traditionally, focusing monochromators consist of rectangular crystal plates mounted on an assembly that allows the orientation of each crystal to be varied in a correlated manner (Bührer, 1994). More recently, elastically deformed perfect crystals (in particular silicon) have been exploited as focusing elements for monochromators and analysers (Magerl & Wagner, 1994).

Since thermal neutrons have velocities that are of the order of km s^{-1}, their wavelengths can be Doppler shifted by diffraction from moving crystals. The k-space representation of the diffraction from a crystal moving perpendicular to its lattice planes is shown in Fig. 4.4.2.3(*a*). This effect is most commonly used in backscattering instruments on steady-state sources to vary the energy of the incident beam. Crystal velocities of 9–10 m s^{-1} are practically achievable, corresponding to energy variations of the order of $\pm$ 60 μeV.

The Doppler shift is also important in determining the resolution of the rotating-crystal time-of-flight (TOF) spectrom-

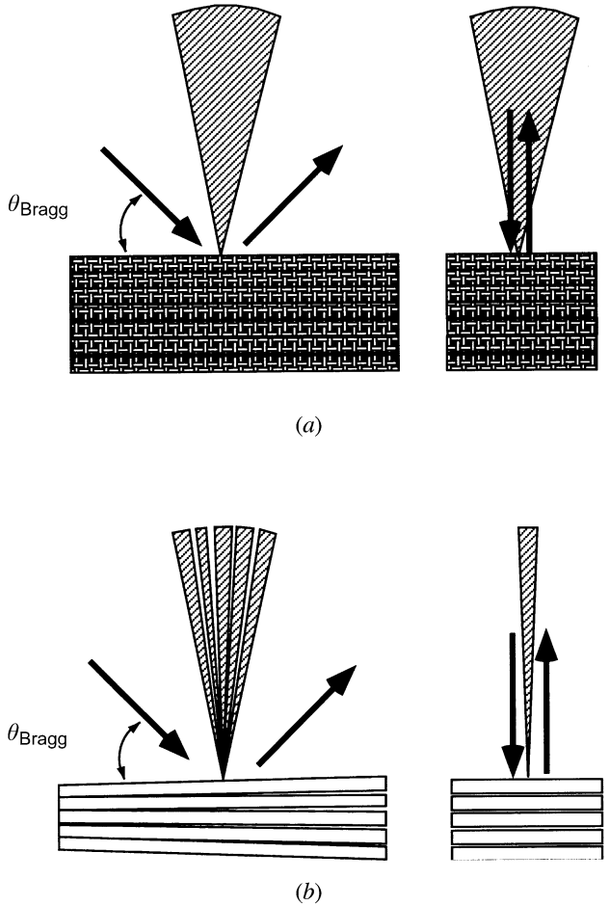

Fig. 4.4.2.1. Two methods by which artificial mosaic monochromators can be constructed: (*a*) out of a stack of crystalline wafers, each with a mosaicity close to the global value. The increase in divergence due to the mosaicity is the same in the horizontal (left picture) and the vertical (right picture) directions; (*b*) out of several stacked thin crystalline wafers each with a rather narrow mosaic but slightly misoriented in a perfectly controlled way. This allows the shape of the reflectivity curve to be rectangular, Gaussian, Lorentzian, *etc.*, and highly anisotropic, *i.e.* vertically narrow (right picture) and horizontally broad (left figure).

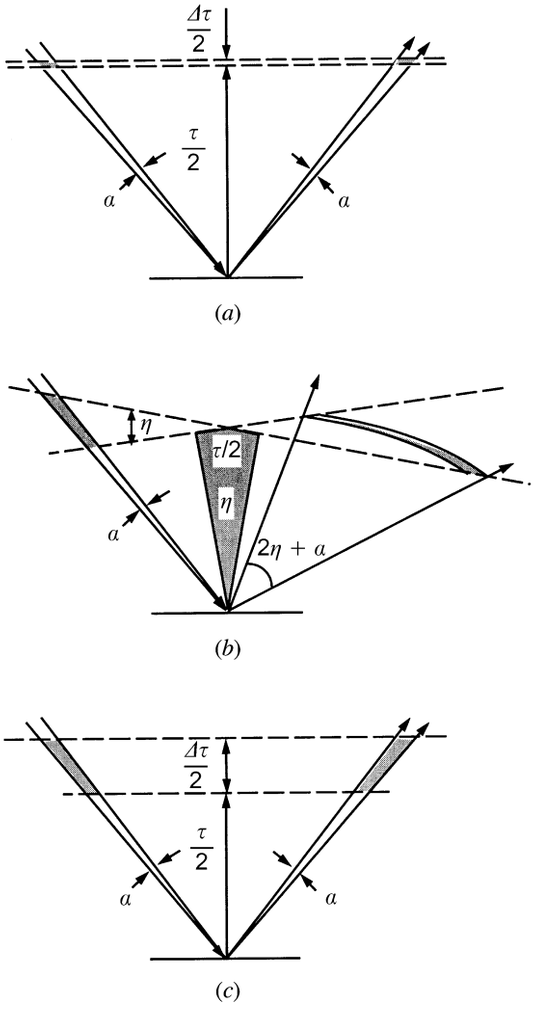

Fig. 4.4.2.2. Reciprocal-lattice representation of the effect of a monochromator with reciprocal-lattice vector τ on the reciprocal-space element of a beam with divergence α. (*a*) For an ideal crystal with a lattice constant width $\Delta\tau$; (*b*) for a mosaic crystal with mosaicity η, showing that a beam with small divergence, α, is transformed into a broad exit beam with divergence $2\eta + \alpha$; (*c*) for a gradient crystal with interplanar lattice spacing changing over $\Delta\tau$, showing that the divergence is not changed in this case.

eter, first conceived by Brockhouse (1958). A pulse of monochromatic neutrons is obtained when the reciprocal-lattice vector of a rotating crystal bisects the angle between two collimators. Effectively, the neutron **k** vector is changed in both direction and magnitude, depending on whether the crystal is moving towards or away from the neutron. For the rotating crystal, both of these situations occur simultaneously for different halves of the crystal, so that the net effect over the beam cross section is that a wider energy band is reflected than from the crystal at rest, and that, depending on the sense of rotation, the beam is either focused or defocused in time (Meister & Weckerman, 1972).

The Bragg reflection of neutrons from a crystal moving parallel to its lattice planes is illustrated in Fig. 4.4.2.3(*b*). It can be seen that the moving crystal selects a larger Δk than the crystal at rest, so that the reflected intensity is higher. Furthermore, it is possible under certain conditions to orientate the diffracted phase-space volume orthogonal to the diffraction vector. In this way, a monochromatic divergent beam can be obtained from a collimated beam with a larger energy spread. This provides an elegant means of producing a divergent beam with a sufficiently wide momentum spread to be scanned by the Doppler crystal of a backscattering instrument (Schelten & Alefeld, 1984).

Finally, an alternative method of scanning the energy of a monochromator in backscattering is to apply a steady but uniform temperature variation. The monochromator crystal must have a reasonable thermal expansion coefficient, and care has to be taken to ensure a uniform temperature across the crystal.

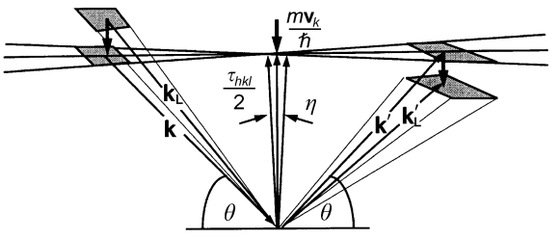

(*a*)

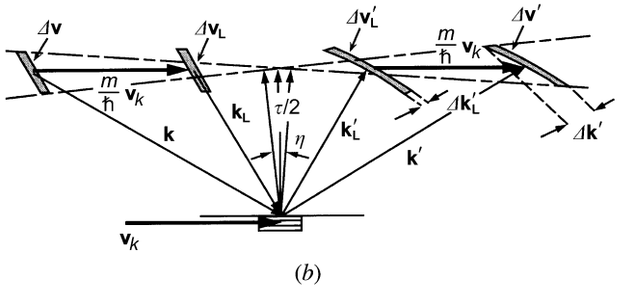

(*b*)

Fig. 4.4.2.3. Momentum-space representation of Bragg scattering from a crystal moving (*a*) perpendicular and (*b*) parallel to the diffracting planes with a velocity $\mathbf{v}_k$. The vectors $\mathbf{k}_L$ and $\mathbf{k}'_L$ refer to the incident and reflected wavevectors in the laboratory frame of reference. In (*a*), depending on the direction of $\mathbf{v}_k$, the reflected wavevector is larger or smaller than the incident wavevector, $\mathbf{k}_L$. In (*b*), a larger incident reciprocal-space volume, $\Delta\mathbf{v}_L$, is selected by the moving crystal than would have been selected by the crystal at rest. The reflected reciprocal-space element, $\Delta\mathbf{v}'_L$, has a large divergence, but can be arranged to be normal to $\mathbf{k}'_L$, hence improving the resolution $\Delta\mathbf{k}'_L$.

Table 4.4.2.2. *Neutron scattering-length densities, Nb_{coh}, for some commonly used materials*

Material	Nb (10^{-6} Å^{-2})
^{58}Ni	13.31
Diamond	11.71
Nickel	9.40
Quartz	3.64
Germanium	3.62
Silver	3.50
Aluminium	2.08
Silicon	2.08
Vanadium	−0.27
Titanium	−1.95
Manganese	−2.95

4.4.2.4. *Mirror reflection devices*

The refractive index, n, for neutrons of wavelength λ propagating in a nonmagnetic material of atomic density N is given by the expression

$$n^2 = 1 - \frac{\lambda^2 Nb_{\rm coh}}{\pi,} \qquad (4.4.2.4)$$

where $b_{\rm coh}$ is the mean coherent scattering length. Values of the scattering-length density $Nb_{\rm coh}$ for some common materials are listed in Table 4.4.2.2, from which it can be seen that the refractive index for most materials is slightly less than unity, so that total external reflection can take place. Thus, neutrons can be reflected from a smooth surface, but the critical angle of reflection, γ_c, given by

$$\gamma_c = \lambda \sqrt{\frac{Nb_{\rm coh}}{\pi}}, \qquad (4.4.2.5)$$

is small, so that reflection can only take place at grazing incidence. The critical angle for nickel, for example, is 0.1° Å^{-1}.

Because of the shallowness of the critical angle, reflective optics are traditionally bulky, and focusing devices tend to have long focal lengths. In some cases, however, depending on the beam divergence, a long mirror can be replaced by an equivalent stack of shorter mirrors.

4.4.2.4.1. *Neutron guides*

The principle of mirror reflection is the basis of neutron guides, which are used to transmit neutron beams to instruments that may be situated up to 100 m away from the source (Christ & Springer, 1962; Maier-Leibnitz & Springer, 1963). A standard neutron guide is constructed from boron glass plates assembled to form a rectangular tube, the dimensions of which may be up to 200 mm high by 50 mm wide. The inner surface of the guide is coated with approximately 1200 Å of either nickel, ^{58}Ni ($\gamma_c = 0.12^\circ$ Å^{-1}), or a 'supermirror' (described below). The guide is usually evacuated to reduce losses due to absorption and scattering of neutrons in air.

Theoretically, a neutron guide that is fully illuminated by the source will transmit a beam with a square divergence of full width $2\gamma_c$ in both the horizontal and vertical directions, so that the transmitted solid angle is proportional to λ^2. In practice, owing to imperfections in the assembly of the guide system, the divergence profile is closer to Gaussian than square at the end of a long guide. Since the neutrons may undergo a large number of reflections in the guide, it is important to achieve a high reflectivity. The specular reflectivity is determined by the surface roughness, and typically values in the range 98.5 to 99% are

references